An optical analysis of the Na^+ influx, of the Ca^{2+} influx and of the action potential shape in the axon initial segment of neocortical pyramidal neurons in a $Na_v1.2$ knock-out mouse

Fatima Abbas, Laila Ananda Blömer, Martina Simonti, Sandrine Cestele, Massimo Mantegazza, Marco Canepari

Univ. Grenoble Alpes, CNRS, LIPhy, F-38000 Grenoble, France

INTRODUCTION

In the intricate world of neuronal activity, $Na_v1.2$ voltage-gated Na^+ channels play a crucial role at the axon initial segment (AIS) of pyramidal neurons for the generation of action potentials (APs). But what occurs on the physiological level when these gates malfunction? To understand the changes associated with these $Na_v1.2$ channelopathies we turned to a heterozygous Scn2a$^{+/-}$ KO mouse model revealing an autistic-like phenotype, memory impairment, and reduced stress reactivity during the third and fourth postnatal weeks. Using ultrafast Na^+, Ca^{2+}, and membrane potential (V_m) imaging, we show a slight reduction in Na^+ influx at the proximal AIS in Scn2a$^{+/-}$ mice compared to their wild-type (Scn2a$^{+/+}$) counterparts. Our findings also highlight an alteration in the Ca^{2+} influx raising the intriguing question of how $Na_v1.2$ loss-of-function affects the AP waveform, particularly within the distal AIS, where $Na_v1.2$ mediates the calcium influx regulating the shape of generating AP.

METHODS

- Experiments were performed on P21-35 C57Bl/6j female mice: heterozygous knockout (Scn2a $^{+/-}$) and wild-type (Scn2a $^{+/+}$)
- Sagittal brain slices from which L5 somatosensory pyramidal neurons were selected

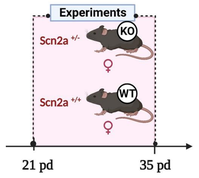

Electrophysiology

- Whole-cell patch clamp to fill the cells with fluorescent indicators: sodium indicator (ING-2), calcium indicator (OGB-5N), or voltage sensitive dye (JPW1114).
- Short current pulses of 3 ms and 1.5 - 2.5 nA amplitude injected through the patch pipette to trigger somatic APs, electrical signals were acquired at 20 kHz.

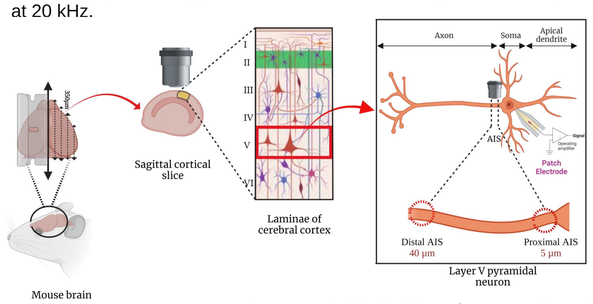

Fluorescent Imaging

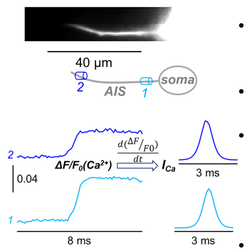

- Images of 64 X 15 µm^2 comprising the axon initial segment (AIS) are acquired at 10 kHz.
- Na^+ and V_m indicators were excited at 520 nm and the Ca^{2+} indicator was excited at 465 nm.
- Signals from proximal and distal areas of the AIS are distinguished.
- Averaged Na^+, Ca^{2+} and V_m data were expressed as fractional changes of fluorescence ($\Delta F/F_0$ signals), calculated after subtraction of the autofluorescence background.
- The time derivative of the fitted Na^+ or Ca^{2+} $\Delta F/F_0$ signal was then calculated.

Reduced sodium current in the proximal part of the AIS in Scn2a$^{+/-}$ mice 1

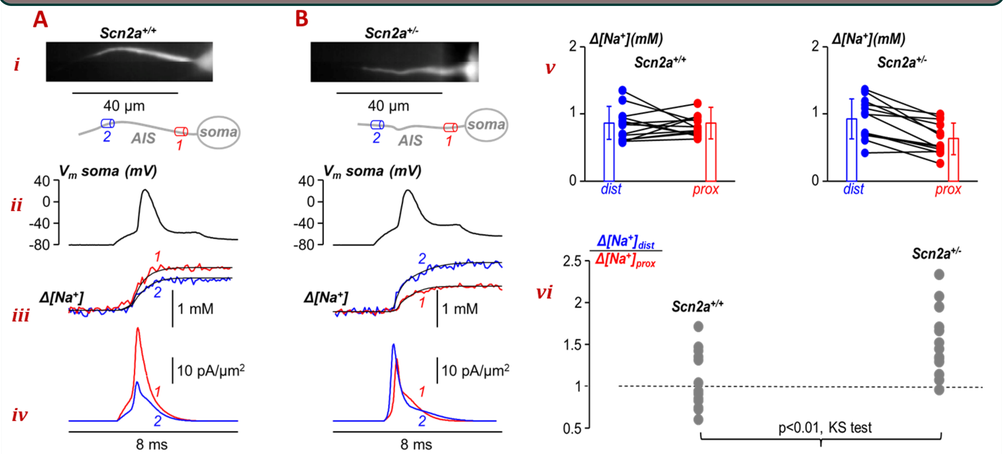

A Example of sodium imaging from WT animals; and KO animals in **B**. (i) Fluorescence image of the AIS and its reconstruction with a proximal (1) and a distal (2) region indicated. (ii) Somatic AP. (iii) Associated corrected Na^+ transients fitted with a model function in 1 and 2. (iv) Na^+ currents calculated from the time-derivative of the Na^+ transient fits. (v) Single cell values of the Na^+ transient maximum in proximal regions and in distal regions (N=26). (vi) Single cell values of the ratio between the maximum distal and proximal Na^+ transients.

In KO, 12 out of 13 cells displayed a reduced sodium influx in the proximal AIS resulting in a positive ratio. Compared to the WT mice, the difference was statistically significant (p=0.007).

Decrease in the delay between the proximal and the distal calcium current peaks in the AIS of Scn2a$^{+/-}$ mice 2

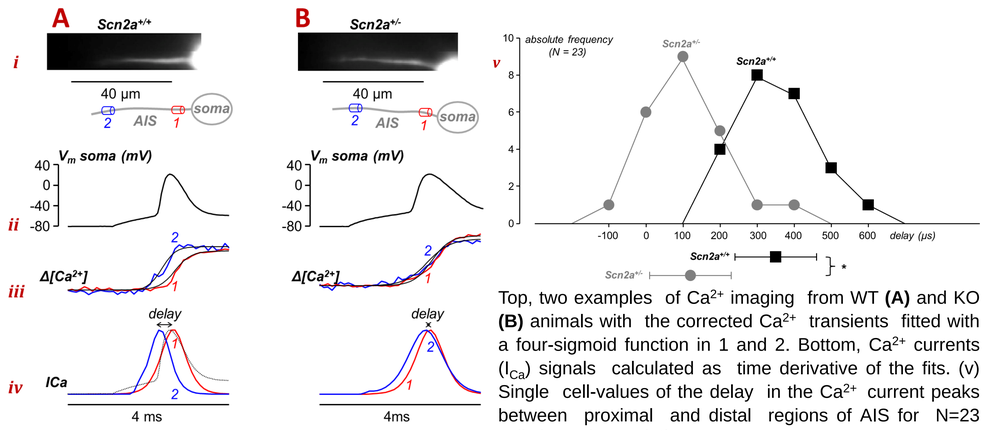

Top, two examples of Ca^{2+} imaging from WT **(A)** and KO **(B)** animals with the corrected Ca^{2+} transients fitted with a four-sigmoid function in 1 and 2. Bottom, Ca^{2+} currents (I_{Ca}) signals calculated as time derivative of the fits. (v) Single cell-values of the delay in the Ca^{2+} current peaks between proximal and distal regions of AIS for N=23 cells in each population.

In contrast to WT, KO animals showed a significantly reduced delay between the proximal and distal I_{Ca} peaks effectively shifting the distal calcium current closer to the proximal one.

Comparative analysis of the AP shape in the AIS Scn2a$^{+/+}$ vs. Scn2a$^{+/-}$ mice 3

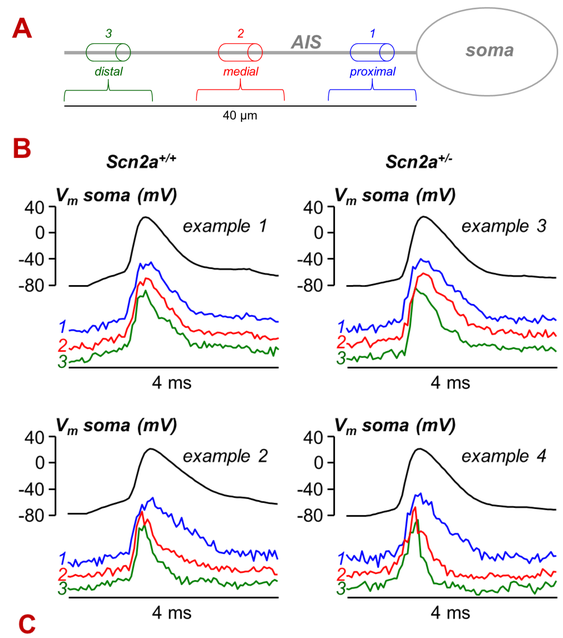

A, Membrane potential imaging (V_m) from three regions of AIS indicated as proximal (1), medial (2), and distal (3).

B, Somatic AP and associated V_m tran sients in 1, 2, and 3 are illustrated in WT Scn2a$^{+/+}$ animals (example 1 and 2) and KO Scn2a$^{+/-}$ animals (example 3 and 4) at a time scale of 4 ms.

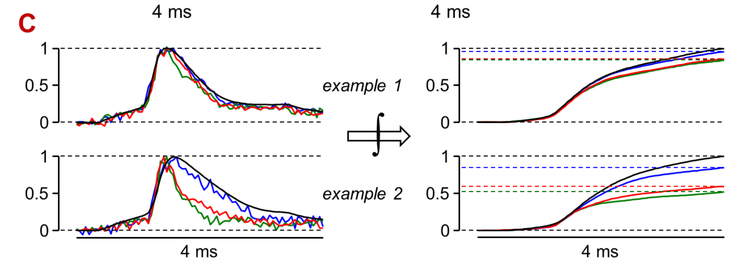

C, Left, somatic and three axonal APs superimposed visually indicated a narrowing of the AP waveform only towards the distal positions of the AIS in Scn2a$^{+/-}$ mouse.

Right, quantitative assessment of this trend (by calculating the V_m integral over 4 ms time window) showing a decreased distal $\int V_m$ maximum in Scn2a$^{+/-}$ mice compared to WT mice (as seen in example 2). D, However, when we analyzed single-cell values of the $\int V_m$ maximum in the proximal, medial, and distal regions across 23 cells from WT and 25 cells from Scn2a$^{+/-}$ mice, this trend did not prove to be statistically significant.

CONCLUSIONS AND FUTURE PERSPECTIVES

Considering the role of $Na_v1.2$ channels as primary mediators of Na^+ influx in the proximal AIS where they are predominantly expressed, as well as their involvement in Ca^{2+} supply in the distal AIS, thereby regulating the initiating AP shape; our optical analyses from haploinsufficient Scn2a$^{+/-}$ mice unveil a disruption in these mechanisms, indicating a reduced number of functional $Na_v1.2$ channels relative to the WT. A comprehensive characterization of this model necessitates further investigation of AP backpropagation. Additionally, our ongoing research extends to exploring a knock-in mouse model of SCN2A LOF channelopathies: Scn2a$^{+/L1314P}$, hoping to provide deeper insights into the underlying mechanisms of these neuronal disorders.